

## **General Disclaimer**

### **One or more of the Following Statements may affect this Document**

- This document has been reproduced from the best copy furnished by the organizational source. It is being released in the interest of making available as much information as possible.
- This document may contain data, which exceeds the sheet parameters. It was furnished in this condition by the organizational source and is the best copy available.
- This document may contain tone-on-tone or color graphs, charts and/or pictures, which have been reproduced in black and white.
- This document is paginated as submitted by the original source.
- Portions of this document are not fully legible due to the historical nature of some of the material. However, it is the best reproduction available from the original submission.

# AgRISTARS

E83-10400  
EW-L3-04402  
JSC-18606

CR-171 682

"Made available under NASA sponsorship  
in the interest of early and wide dis-  
semination of Earth Resources Survey  
Program information and without liability  
for any use made thereof."

## Early Warning and Crop Condition Assessment

A Joint Program for  
Agriculture and  
Resources Inventory  
Surveys Through  
Aerospace  
Remote Sensing

MARCH, 1983

### Metsat Information Content:

CLOUD SCREENING AND SOLAR CORRECTION INVESTIGATIONS  
ON THE INFLUENCE OF NOAA-6 ADVANCED VERY HIGH  
RESOLUTION RADIOMETER DERIVED VEGETATION ASSESSMENT

(E83-10400) METSAT INFORMATION CONTENT: N83-34393  
CLOUD SCREENING AND SOLAR CORRECTION  
INVESTIGATIONS ON THE INFLUENCE OF NOAA-6  
ADVANCED VERY HIGH RESOLUTION RADIOMETER  
DERIVED VEGETATION (Lockheed Engineering and G3/43 00400  
Unclas

Mike L. Mathews

Lockheed Engineering and Management  
Services Company, Inc.



Lyndon B. Johnson Space Center  
Houston, Texas 77058

1. Report No. EW-L3-04402;JSC-18606		2. Government Accession No.		3. Recipient's Catalog No.	
4. Title and Subtitle Metsat Information Content: Cloud Screening and Solar Correction Investigations on the Influence of NOAA-6 Advanced Very High Resolution Radiometer Derived Vegetation Assessment				5. Report Date March 1983	
				6. Performing Organization Code	
7. Author(s) Mike L. Mathews Lockheed Engineering and Management Services Co., Inc.				8. Performing Organization Report No. LEMSCO - 19199	
				10. Work Unit No.	
9. Performing Organization Name and Address Lockheed Engineering and Management Services Co., Inc. 1830 NASA Road 1 Houston, Texas 77258				11. Contract or Grant No. NAS 9-15800	
				13. Type of Report and Period Covered Technical Report	
12. Sponsoring Agency Name and Address Early Warning/Crop Condition Assessment Project Office USDA, 1050 Bay Area Blvd. Houston, Texas 77058      Tech Monitor: V. S. Whitehead				14. Sponsoring Agency Code	
15. Supplementary Notes The Agriculture and Resources Inventory Surveys Through Aerospace Remote Sensing is a joint program of the U.S. Department of Agriculture, the National Aeronautics and Space Administration, the National Oceanic and Atmospheric Administration (U.S. Dept. of Commerce), the Agency for International Development (U.S. Dept. of State), and the U.S. Dept. of the Interior.					
16. Abstract This document describes the development of the cloud indicator index (CII) for use with Metsat's advanced very high resolution radiometer (AVHRR). The CII is very effective at identification of clouds. Also, explored in this document are different solar correction and standardization techniques and the impact of these corrections have on the information content of AVHRR data.					
17. Key Words (Suggested by Author(s)) Environmental Vegetation Index (EVI) Cloud Indicator Index (CII) AVHRR                      Cloud Screening Metsat                      Solar corrections NOAA-6				18. Distribution Statement	
19. Security Classif. (of this report) Unclassified		20. Security Classif. (of this page) Unclassified		21. No. of Pages 42	
				22. Price*	

\*For sale by the National Technical Information Service, Springfield, Virginia 22161

ORIGINAL PAGE IS  
OF POOR QUALITY

EW-L3-04402  
JSC-18606

METSAT INFORMATION CONTENT:

CLOUD SCREENING AND SOLAR CORRECTION INVESTIGATIONS  
ON THE INFLUENCE OF NOAA-6  
ADVANCED VERY HIGH RESOLUTION RADIOMETER  
DERIVED VEGETATION ASSESSMENT

Job Order 72-457

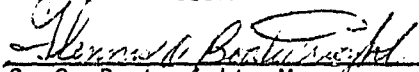
This report describes activities of the  
Early Warning/Crop Condition Assessment Project  
of the AgRISTARS program

Prepared by

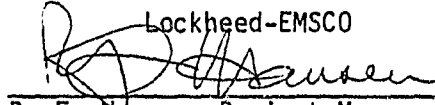
Mike L. Mathews

Approved by

USDA

  
G. O. Boatwright, Manager  
Early Warning/Crop Condition  
Assessment Project, AgRISTARS  
Program

Lockheed-EMSCO

  
R. F. Hansen, Project Manager  
Early Warning/Crop Condition  
Assessment Project,  
Renewable Resources Department

LOCKHEED ENGINEERING AND MANAGEMENT SERVICES COMPANY, INC.

UNDER CONTRACT NAS 9-15800

for

EARTH RESOURCES APPLICATIONS DIVISION  
SPACE AND LIFE SCIENCES DIRECTORATE

NATIONAL AERONAUTICS AND SPACE ADMINISTRATION  
LYNDON B. JOHNSON SPACE CENTER  
HOUSTON, TEXAS

MARCH 1983

LEMSCO-19199

## PREFACE

The Agriculture and Resources Inventory Surveys Through Aerospace Remote Sensing is a multiyear program of research, development, evaluation, and application of aerospace remote sensing for agricultural resources, which began in fiscal year 1980. This program is a cooperative effort of the U.S. Department of Agriculture, the National Aeronautics and Space Administration, the National Oceanic and Atmospheric Administration (U.S. Department of Commerce), the Agency for International Development (U.S. Department of State), and the U.S. Department of the Interior.

## TABLE OF CONTENTS

Page	
1. INTRODUCTION . . . . .	1-1
1.1 Background . . . . .	1-3
1.2 Scope . . . . .	1-5
1.3 Assumptions and Constraints . . . . .	1-6
1.4 Study Area . . . . .	1-7
2.0 METSAT AND METSAT DERIVED VEGETATION INDEX NUMBERS . .	2-1
2.1 POES Operational Data Flow . . . . .	2-1
2.2 Metsat Derived Indexes . . . . .	2-4
2.2.1 Environmental vegetation index . . . . .	2-4
2.2.2 Normalized vegetation index . . . . .	2-5
2.2.3 Cloud indicator index . . . . .	2-6
3.0 ANALYTICAL PROCEDURES . . . . .	3-1
3.1 Preliminary Investigations . . . . .	3-1
3.2 Database Development . . . . .	3-3
3.3 Statistical and Graphical Analysis . . . . .	3-4
4.0 RESULTS AND CONCLUSIONS . . . . .	4-1
4.1 Identification of Cloud Contaminated Cells . . . . .	4-1
4.2 Effects of Solar Corrections/ Standardization on the EVI . . . . .	4-8
4.3 Mean and Variances Equality Tests . . . . .	4-11
5.0 LITERATURE CITED . . . . .	5-1

## TABLES

Table		Page
2-1	A comparison of selected characteristics of Landsat's multispectral scanner (MSS) and Metsat's advanced very high resolution radiometer (AVHRR) in the local area coverage (LAC) mode.	2-2
4-1	Cloud density codes and their derivations. The cloud code assigned to an IJ grid cell was dependent on the K/I ratio; i.e. the ratio of the remaining pixels after applying a threshold to the total number of pixels in the cell.	4-2
4-2	This table is a summary of descriptive statistics for the three types of unscreened (a) and screened (b) EVI VIN's for the July observations, over Illinois.	4-16

## FIGURES

Figure	Page
1-1 This plot shows the highly variable scene mean EVI's, uncorrected, over the Illinois study site in July, 1980.	1-4
1-2 The study cells. This site consists of 81 IJ grid cells, as shown, in the southern three quarters of Illinois.	1-8
4-1 A graph of the cloud indicator index, calculated from channels 3 and 4 against the cloud density code, computed from a threshold base on channels 1 and 2. The greater the positive cloud density code the greater the number of cloud contaminated pixels within a cell. Notice that a secondary ordinate placed at CII=37.0 places most of the cloud contaminated cells to the left (CII<37.0) and most of the contaminated cells to the right (CII>37.0). Refer to table 4.1 for an explanation of the cloud density code.	4-3
4-2 (a) - a graph of midcell pixel numbers against EVI's calculated from the July channel means, n = 648 (b) is the same July EVI against midcell pixel numbers with a CII threshold of $\leq 37.0$ and a midcell pixel number threshold of $\leq 200$ , n = 312. Notice the reduction of variability of the EVI graph (b) compared to graph (a).	4-5
4-3 Plots of the July Channel 1 cell means against channel 2 cell means without (a) and with (b) thresholds of CII $\leq 37.0$ and midcell pixel number $\leq 200$ . Notice how the bulk of the tightly clustered data with low reflectance in channels 1 and 2 remained after thresholds were applied and the less clustered more amalgamous data has been omitted.	4-7
4-4 Plots of the July channel 3 cell means against channel 4 cell means without (a) and with (b) thresholds of CII $\leq 37.0$ and midcell pixel numbers $\leq 200$ . Notice how the bulk of the tightly clustered data remained after the thresholds were applied and the amalgamous data has been omitted.	4-9



- 4-5 These plots show the EVI plotted against the midcell pixel number to illustrate the distribution changes as different solar correction/standardization techniques are applied. All plots use the screened July data for illustration. The EVI is uncorrected and unstandardized in (a); the standard Landsat MSS correction ( $1.0/\cos \theta$ ) has been applied in (b); and the EVI has been solar corrected and standardized to  $39^\circ$  in (c). Note how the EVI becomes increasingly more biased as corrections and standardizations are applied. 4-10
- 4-6 The above tables show the results from the tests of equality between variances (a) and means (b) at the  $\alpha = 0.05$  level of significance for unscreened and uncorrected EVI's in July, 1980. Note: \* - indicates means or variances are significantly different and the null hypothesis of equality should not be accepted; NS - denotes no significant difference and the null hypothesis should be accepted. 4-12
- 4-7 The above tables show the results from the tests of equality between variances (a) and means (b) at the  $\alpha = 0.05$  level of significance for screened and uncorrected EVI's in July 1980. Note: \* - indicates means or variances are significantly different and the null hypothesis of equality should not be accepted; NS - denotes no significant difference and the null hypotheses should be accepted. 4-13
- 4-8 A plot of screened and unscreened scene mean EVI's over the Illinois study site by date for the July data only. July 9th and 10th screened EVI's are not plotted as only 3 and 6 observations, respectively, were left after screening. 4-15

CLOUD SCREENING AND SOLAR CORRECTION INVESTIGATIONS ON THE  
INFLUENCE OF NOAA-6 ADVANCED VERY HIGH RESOLUTION RADIOMETER  
DERIVED VEGETATION ASSESSMENT

1. INTRODUCTION

The use of remotely sensed data to identify, mensurate and assess terrestrial landcover has accelerated exponentially since the end of World War II. Black and white and black and white infrared aerial photography progressed to color and color infrared photography along with improvements in film resolution. Aircraft which were able to obtain increasingly higher altitudes offered greater areal coverage of the earth's surface. Subsequent terrestrial and atmospheric remote sensing instruments evolved to aircraft and spacecraft borne analog and digital scanners, radars and cameras with superior radiometric, spatial and temporal resolution. The Earth Resources Technology Satellite (ERTS), launched in 1972, housed a return beam vidicom (RBV) and a multispectral scanner (MSS). These instruments were intended to provide useful and timely data to analyze landcover throughout the globe. ERTS was later renamed Landsat as the system evolved in sophistication.

The National Aeronautics and Space Administration (NASA) implemented the Large Area Crop Inventory Experiment (LACIE) primarily to identify and inventory world wheat production using Landsat MSS data. One significant conclusion of the experiment was that global vegetation conditions could be monitored with MSS data (NASA, 1978). Following LACIE the Agriculture and Resources Inventory Surveys Through Aerospace Remote Sensing (AgRISTARS) project was implemented to research, develop, evaluate, and apply aerospace

remote sensing for agricultural resources. Through the AgRISTARS program, with its multi-agency participation, the National Oceanic and Atmospheric Administration (NOAA) meteorological satellites (Metsat) were found to be useful for determining environmental conditions (Gray and McCrary, 1981). The first Metsat was the Television Infrared Observation Satellite (TIROS) which was launched in 1960. Additional instrumentation and new techniques have been incorporated in later Metsats which not only provided increased weather information but also provided excellent data for other disciplines as well (Horvath, et al, 1982). The most current Metsats, NOAA-6 and NOAA-7, have onboard four sensor systems; the Advanced Very High Resolution Radiometer (AVHRR), the TIROS Operational Vertical Sounder (TOVS), the Data Collection System (DCS), and the Space Environmental Monitor (SEM). The primary sensor, the AVHRR, operates in a global area coverage (GAC) mode or a local area coverage (LAC) mode and can provide real-time transmission or digital tape recordings for playback at a later time (Gray, et al, 1981).

NOAA-6 and NOAA-7 AVHRR sensors provide daily (occasionally twice daily) coverage for any given point on the earth's surface at a resolution, at nadir, of one kilometer for LAC and four kilometers for GAC. Landsat's MSS sensor provides 18 day (9 day when two satellites are in operation) coverage for any given location at a resolution of 79 meters (.079 km). This contrast in sensor coverages and resolution provides exceptional temporal and spatial data for environmental analysis.

The Early Warning and Crop Condition Assessment Project of the AgRISTARS program is using the temporal/resolution contrast between Metsat and Landsat in research to develop and test techniques which will make possible

or enhance operational methodologies for crop condition assessment. The results of this research will be used primarily by the Foreign Agriculture Service (FAS) of the USDA which is responsible for providing early warning of changes which may affect foreign crop production, its quality, and for assessing crop conditions (NASA, 1982).

This paper presents results obtained under task fourteen; effects of spatial resolution on information content, which is under the Spectral Analysis and Assessment project of the 1982-83 Project Implementation Plan for the Early Warning and Crop Condition Assessment Project of AgRISTARS (Boatwright, 1981). Specifically this paper shows how adverse effects on vegetative index numbers derived from Metsat AVHRR data can be reduced.

### 1.1 Background

Vegetation index numbers derived daily from NOAA-6 exhibit a high degree of variability as seen in Figure 1-1. The accuracy of an index will always be questionable to some extent but an index should be precise. Figure 1-1 shows that within-the-scene daily fluctuations in the data are not precise nor can they be accurate.

There also exists the question of daily comparability. Should some method of relative standardization be employed to compare indexes that are temporarily separate? An index being used to monitor crop conditions through the year should be reliable from one observation to the next. If conditions are near identical between two observations the indexes should also be near

ORIGINAL PAGE 15  
OF POOR QUALITY

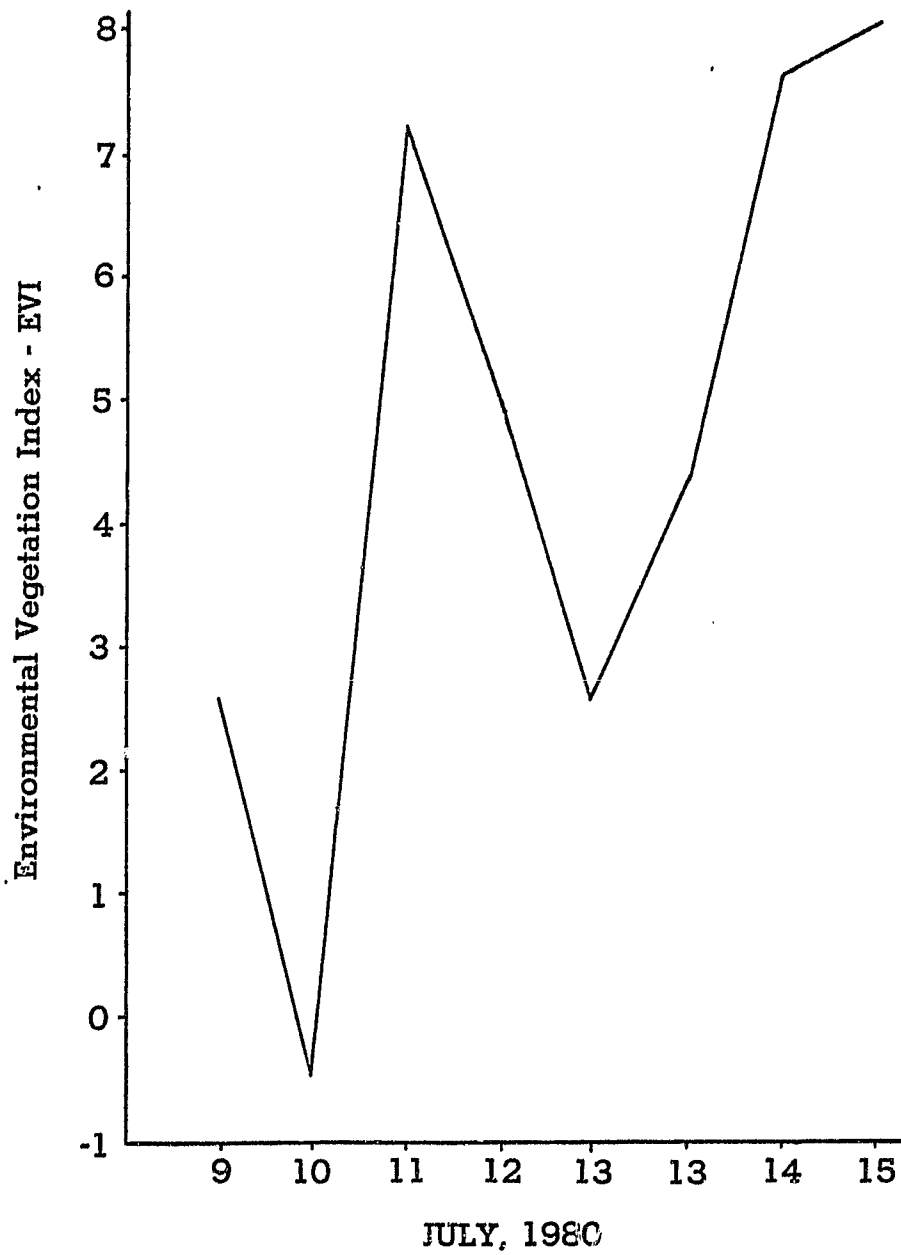


Figure 1-1. This plot shows the highly variable scene mean EVI's, uncorrected, over the Illinois study site in July, 1980.

identical for that crop regardless of satellite position, sun position or atmospheric conditions.

Horvath, et al, (1982) presents a comprehensive study of channels one and two of NOAA-6 AVHRR data. This study has indications of index instability. Apparent from this study, the greatest amount of instability can be attributed to clouds in the scene.

## 1.2 Scope

This paper documents the efforts conducted to establish a method to identify adverse effects on AVHRR derived vegetative index numbers (VINs). Once these adverse effects were identified, procedures were established to correct or remove these adverse effects on AVHRR derived VINs. These procedures should be easily implemented on the operational data base of the USDA Foreign Agriculture Service.

### 1.3 Assumptions and Constraints

Procedures developed during this study are intended to be implemented on the USDA Foreign Agriculture Service's (FAS) operational data base (CADRE)\*, hence, the major constraint is working within the IJ grid system that CADRE is spatially divided into. Over the study area these IJ grid cells are approximately 25 nautical miles square. All vegetation index numbers, model estimates, crop condition assessments or soil moisture conditions are all reduced to these 625 square nautical mile IJ grid cells. Because of the enormous size of the database spatial elements, one assumption made was any given IJ grid cell cannot significantly change in one day. Perhaps during the course of a week an area the size of an IJ grid cell can change. One exception to this assumption would be any adverse event. These events include rainstorms, snowstorms, high winds, etc.

Another assumption that must be made is that the AVHRR sensor provides stable radiometric data. With these assumptions in mind, any adverse effect on AVHRR data and subsequent indexes are due to atmospheric conditions, sensor scan angles, and/or solar zenith angles.

---

\* CADRE - Crop Assessment Data Retrieval and Evaluation Database

#### 1.4 Study Area

The study area lies nearly completely in the southern three-quarters of the state of Illinois. The study area consists of 81 1/2 grid cells arranged in a seven by eleven pattern with two additional cells on the north side of the northwest corner of the seven by eleven grid area and two additional cells on the east side of the northeast corner as shown in Figure 1-2. The study area also contains small portions of Missouri, Kentucky, Indiana and Iowa.

The natural vegetation of the area consists primarily of Oak-Hickory forests and Bluestem prairie with smaller amounts of Oak-Hickory-Pine forest and Southern floodplain forests in the southern portion of the study site. Commercial agricultural use includes cropland in the central and northeastern areas and cropland with pasture and forests in the southern and western portion of the study area. Specifically, corn is the dominant crop type grown north of an east-west line through the St. Louis vicinity and wheat is primarily grown south of the line (Horvath, et al, 1982).

Major physiographic features consist of smooth plains in the central and northeastern portions where the majority of the corn crop is grown. The southern and western areas consist of irregular plains where the primary wheat production is located. Topographic relief ranges from 500 to 1000 feet above sea level.



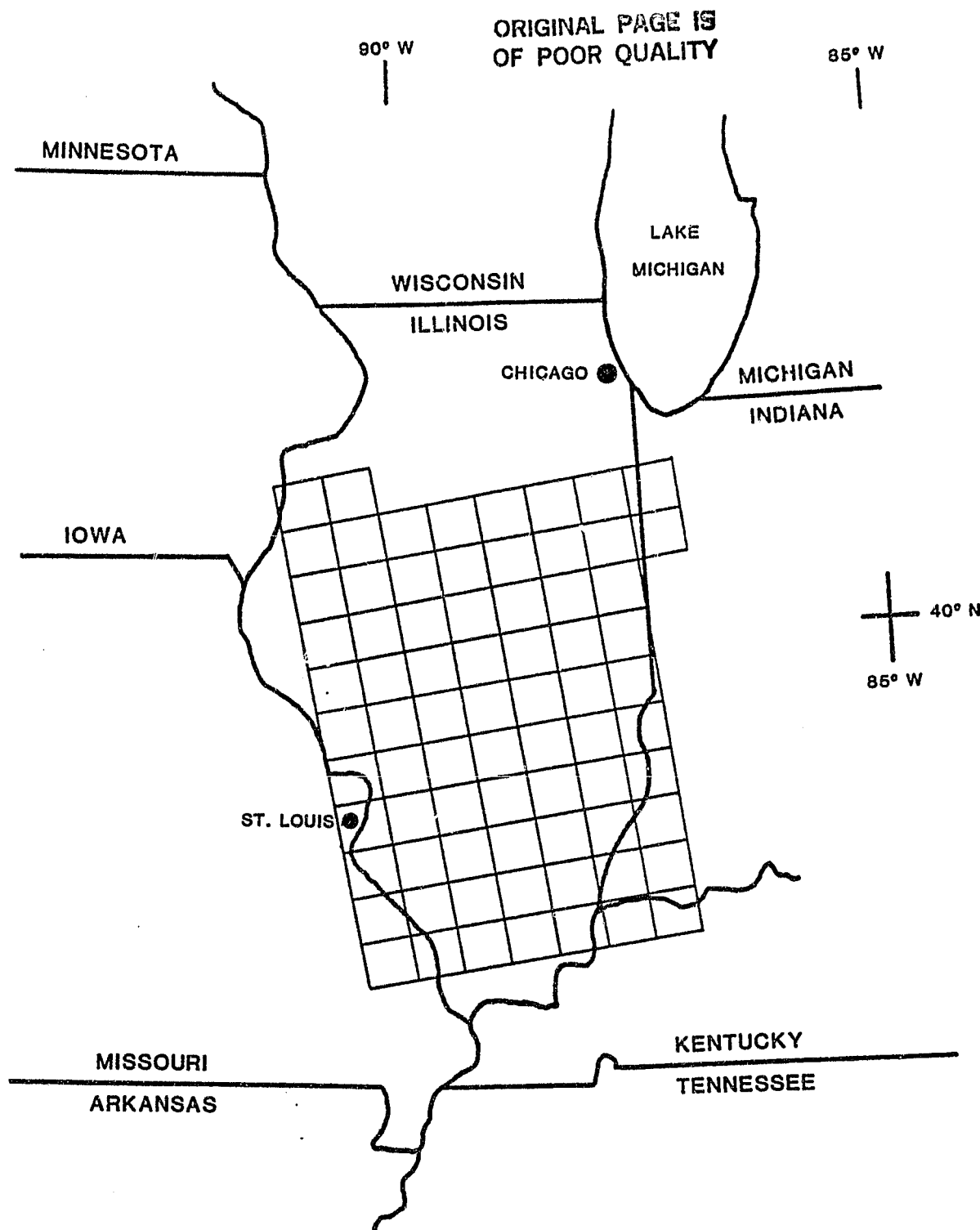


Figure 1-2. The study cells. This site consists of 81 IJ grid cells, as shown, in the southern three-quarters of Illinois.

## 2.0 METSAT AND METSAT DERIVED VEGETAL INDEX NUMBERS

Indexes to indicate standing green biomass quantity and/or quality were first determined (and still are) from remote platforms with aerial photography. However, vegetation index numbers (VINs) are usually associated with Landsat MSS data. Recently though, VINs have been derived from Metsat data (Gray and McCrary, 1981). This section discusses some of the attributes of Metsat and the VINs derived from Metsat AVHRR data.

### 2.1 POES Operational Data Flow

Polar orbiting environmental satellites\* (POES) have been operational since October 1978. The POES system is operationally designed to monitor global atmospheric phenomena. There are contrasting as well as complementary attributes of both the Landsat MSS and Metsat AVHRR (See table 2-1). Landsat MSS data is reflective in all four channels while Metsat AVHRR is reflective in two channels, emmitive in one channel and both reflective and emmitive in one channel. (Note: there is no sensible reflected energy during a nighttime pass). Because of the success of establishing VIN's with Landsat MSS data (reflective) the Early Warning and Crop Condition Assessment project of AgRISTARS has explored the utility of using the reflective channels of NOAA-6 and NOAA-7 to derive VIN's with greater frequency and at a coarser resolution.

---

\*POES is a term to designate a family of satellites based on TIROS-N. This family includes TIROS-N, NOAA-6 and NOAA-7 meteorological satellites, Metsats.

Table 2-1 - A comparison of selected characteristics of Landsat's multi-spectral scanner (MSS) to Metsat's Advanced Very High Resolution Radiometer (AVHRR) in the local area coverage (LAC) mode.

CHARACTERISTIC	LANDSAT (MSS)	METSAT (AVHRR)
Spectral Band Response ( $\mu$ m)	1: 0.50 - 0.60 2: 0.60 - 0.70 3: 0.70 - 0.80 4: 0.80 - 1.10	1: 0.55 - 0.70 2: 0.70 - 1.10 3: 3.55 - 4.00 4: 10.50 - 11.50
Ground Resolution (IFOV)	79 M	1100 M
Scan Width (FOV)	185 kM ( $\pm 5.78^\circ$ )	2900 kM ( $\pm 55.4^\circ$ )
Temporal Coverage	18 day	1 day
Altitude	920 kM	832 kM

The following steps are taken to make NOAA-6 AVHRR LAC data available to be processed at the Early Warning and Crop Condition Assessment project office in Houston, Texas.

- The AVHRR sensor onboard NOAA-6 receives spectral data and records or transmits digital counts.
- Data counts are received and recorded on high density digital tapes (HDDT) at Wallops Island, Virginia; Gilmore Creek, Alaska; San Francisco, California or Honolulu, Hawaii.
- The data on HDDT's are then sent by microwave transmission to NOAA's National Meteorological Center in Suitland, Maryland where the HDDT's are processed into LAC and GAC tapes by the National Environmental Satellite and Data Information Service (NESDIS) of NOAA which is responsible for archiving and distributing LAC and GAC digital tapes.
- Digital LAC tapes are received by the Early Warning Crop Condition Assessment project office in Houston, Texas where they are displayed and reviewed for quality and areas of interest.
- Acceptable tapes or portions of tapes are processed onto the USDA Foreign Agriculture Service's PDP 11/70 disk files which are divided into IJ grid cells\* of interest.
- These disk files are further processed to compute VIN's, etc., based on user requirements.

The above steps are completed within five to ten days thus facilitating near real time processing.

\*IJ grid cells are derived from dividing a polar stereographic projection of each hemisphere into 512 by 512 cells. Dimensions of the cells range from 29 miles square near the poles to 14 miles square near the equator (Charney and Phillips, 1953).

## 2.2 Metsat Derived Indexes

In either an operational or research mode there are three common indexes calculated using four channel AVHRR data. The following briefly discusses the theory behind each index and illustrates its calculation.

### 2.2.1 Environmental vegetation index

The environmental vegetation index\* (EVI) is the difference between the infrared reflectance (Channel 2) and the visible reflectance (Channel 1). A complete discussion is presented by Horvath, et al, (1982). Mathematically:

$$EVI = R_2 - R_1$$

where  $R_2$  and  $R_1$  represent the reflectance derived from channel two and channel one, respectively. There are also two commonly used derivations of the EVI. One derivation of the EVI is the solar corrected EVI ( $EVI_{corr}$ ). The solar correction, one over the cosine of the solar zenith angle, is a commonly applied solar correction used with Landsat and is calculated:

$$EVI_{corr} = (R_2 - R_1) * (1.0/\cos \theta)$$

---

\* Also known as GMI (Gray-McCrary Index)

where  $\theta$  is the solar zenith angle. The other derivation of the EVI is the standardized/solar corrected EVI (EVI\*) where the solar corrected EVI is standardized to a common look angle, usually 39 degrees, that of Landsat. The EVI\* is calculated:

$$EVI^* = (R_2 - R_1) * (1.0 / \cos \theta) * (\cos \emptyset / \cos \theta)$$

where  $\emptyset$  is the standard angle.

#### 2.2.2 Normalized vegetation index

The Normalized Vegetation Index (NVI) was an attempt to reduce between scene variability in VIN's. The principle of this VIN calculation is based on the idea of mathematical standardization which is to substitute this normalized ratio for reflectance (Cate, et al, 1981). The NVI is calculated:

$$NVI = (R_2 - R_1) / (R_2 + R_1)$$

where  $R_2$  and  $R_1$  is the reflectance derived from channel two and channel one, respectively.

### 2.2.3 Cloud indicator index

The cloud indicator index (CII)\* is calculated from the thermal channels. Channel four is a direct measure of radiant temperature of the emitting target. Channel three is composed of both reflective and emissive components. Also, the channel three band width covers a water absorption window. Complete exhaustive analysis of channels three and four is currently underway and is beyond the scope of this project. However, the CII is believed to be useful in identification of clouds. It is assumed the Channel three transformation is a general measure of wetness and channel four is a general measure of temperature. Therefore, cold, wet objects (clouds) are identifiable using this index. The CII is the difference between channel four and channel three:

$$CII = E_4 - (100 * E_3)$$

where  $E_4$  and  $E_3$  are the energy in milliwatts per square meter per steradian per centimeter as derived from channel four and channel three counts respectively.

---

\* Also known as the McCrary-Gray Index (MGI)

### 3.0 ANALYTIC PROCEDURES

The data acquired for this study is the complete set of data originally used by Horvath, et al, (1982) to investigate the reflective channels of Metsat's AVHRR. Horvath, et al, indicated this representative data set possessed some instability diurnally as well as daily. This study was also in support of a study to determine the information content using variable pixel (cell) sizes. A detailed statistical investigation is beyond the scope of this study because during the preliminary analysis stage, and since, the NOAA-6 AVHRR sensor has failed to provide significant data. The NOAA-7 AVHRR sensor has completely replaced, rather than supplement, NOAA-6 AVHRR data and the satellite attributes are of such a difference only a cursive investigation is within the scope in order to identify "universal" situations or conditions which may be transferable to NOAA-7 and NOAA-8 technology.

#### 3.1 Preliminary Investigations

The dataset used for a cursory examination covered the dates July 9, 1980 to July 15, 1980, with two observations on July 13, 1980; October 8, 1980 and October 10, 1980 through October 12, 1980. This dataset consisted of the EVI\*, I and J grid numbers, the date, solar zenith angle and pixel numbers for the cell center and I-and K-counts. I-counts are a count of all the pixels in a given IJ grid cell. K-counts are a count of the pixels used in the calculation of the EVI\* for a grid cell. The difference between I-counts and K-counts is the number of pixels omitted by the thresholding technique used. Later investigations were unable to identify



the thresholding technique used. However, this thresholding technique was originally intended to identify pixels containing clouds and visually appeared to do so.

Classical statistical t and F tests were performed on the scene means and variances, using this dataset, testing to find which, if any, adjacent dates have the same statistical mean and/or variance. Considering only the eight observations in July, 1980 and assuming the scene cannot significantly change from day to day only three variances and none of the means of the scene EVI\*'s were statistically the same.

From a visual interpretation of the histograms of EVI\*'s it is evident that essentially cloud free days (July 14, July 15) present a near normal distribution. However, dates containing substantial amounts of clouds (July 9 and July 10) exhibit a definite bi-model distribution of EVI\*'s.

From scatterplots of nearly every variable combination in this small dataset evidence was found which indicated thresholds exist to identify clouds. Also, there seemed to be unexplained trends in the scatterplots.

The above explained relationships provided enough evidence to warrant development of a complete computer compatible data base for further analysis.

### 3.2 Data Base Development

Due to the inability to identify the thresholds applied to Channel one, Channel two or the subsequent EVI\* used in the cursory examination, a new data base was developed over the same area during the same dates which contained data with no thresholds applied. The data base consists of:

- the julian date,
- I and J cell numbers,
- the mean for each of the four channels per IJ grid cell with Channels one and two in percent reflectance and channels three and four in degrees Kelvin,
- the solar zenith angle at the IJ cell center,
- the pixel number at the IJ cell center,
- the K/I ratios,
- the minimum and maximum daily temperatures, and
- the daily precipitation.

This data base lends itself well to the calculation of EVI,  $EVI_{corr}$ , EVI\*, NVI and CII with or without thresholding or correcting of the values.

### 3.3 Statistical and Graphical Analysis

The approach to the analysis of this data has been kept reasonably simple for two reasons. First, the NOAA-6 AVHRR sensor has not provided useful data since the summer of 1982. Secondly, significant findings from this analysis intend to be easily implemented on an operational global vegetation analysis system by the USDA Foreign Agricultural Service. To keep within the intended scope of this study, a simple examination of the spectral profile should suffice. Assessment of data information content was based on such an examination.

Student t statistics were computed to test equality of the scene means between all possible dates, with particular attention given to consecutive acquisition dates. Null hypotheses of equal means between all possible dates with an acceptance level of five percent (two tail) was used. Also, F statistics were computed to test variance equality for all possible dates. Null hypotheses of equal variances between all possible dates with an acceptance level of five percent (two tail) was used. It was necessary to complete variance equality tests first in order to select the proper equation to use when testing the means. The tests of means and variances were computed on the data set as it was and also after any application of thresholding techniques. This gave an indication of how the sample distribution behaved before and after thresholding procedures were applied.

Scatterplots were generated for many combinations of variables to identify relationships that could be used to identify and eliminate adverse effects on the AVHRR derived VIN's. Scatterplots were regenerated using the thresholding techniques to verify the utility of the threshold.

Scatterplots were also generated to determine what effect, if any, solar corrections had on the information content of the data or the corrected VINs.

## 4.0 RESULTS AND CONCLUSIONS

This section discusses the significant findings related to information content of NOAA-6 AVHRR data. Methods to screen data for cloud contamination based on the spectral profile were established. Effects of solar correcting algorithms were determined. Also shown in this section are the results of the statistical tests describing the population before and after screening techniques were applied.

### 4.1 Identification of Cloud Contaminated Cells

The database contained two complementary variables, namely the cloud density code (CDC) and the cloud indicator index (CII). The cloud density code was derived from a previous iteration of the database from K/I ratios. The K/I ratio was the ratio of the number of pixels which passed some undefined threshold to the total number of pixels in an IJ grid cell. This ratio was then coded using the coding scheme shown in table 4.1. The threshold was used by the USDA Foreign Agricultural Service to identify clouds and other amalgomous non-vegetal features based on the EVI of each pixel. The CII, however, is intended to identify clouds based on the thermal channel means of each IJ cell. Figure 4.1 shows a plot of the cloud density code versus the cloud indicator index. Figure 4.1 also shows that a CII in the range from 30 to 40 will put the majority of the cloud contaminated cell numbers at less than 30 to 40 while uncontaminated cells would have index numbers greater than 30 to 40. A CII of 37.0 (second ordinate in figure 4.1) gave the best visual separation between the cloud

Table 4.1 - Cloud codes and their derivations. The cloud code assigned to an IJ grid cell was dependent on the K/I ratio; i.e., the ratio of the remaining pixels after applying a threshold to the total number of pixels in the cell.

CLOUD CODE	K-I RATIO RANGE (percent)
0*	.9998 - 1.000 no clouds
1	.9875 - .9997
2	.8125 - .9374
3	.6875 - .8124
4	.5625 - .6874
5	.4375 - .5624
6	.3125 - .4374
7	.1875 - .3124
8	.0625 - .1874
9	.0000 - .0624 completely cloud covered

\* a cell which had been assigned a code of zero was changed to -2 if any of the neighboring cells had a cloud code equal to 1, if any neighboring cells had codes greater than 1 the cell was assigned the value -1. The code of zero remained if none of the neighboring cells contained cloud codes.

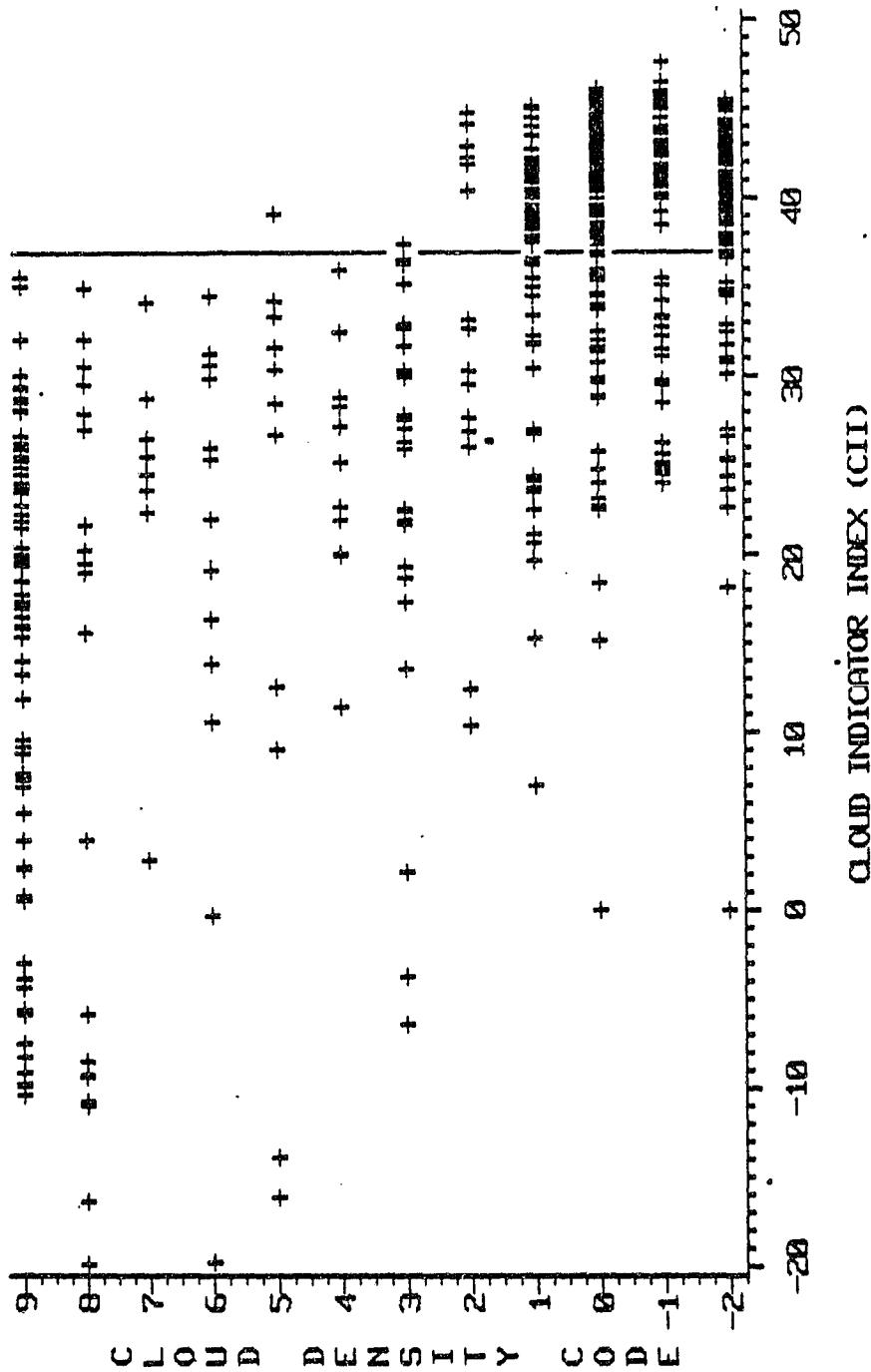


Figure 4.1 - A graph of the cloud indicator index, calculated from channels 3 and 4 against the cloud density code, computed from a threshold based on channels 1 and 2. The greater the positive cloud density code the greater the number of cloud contaminated pixels within a cell. Notice that a secondary ordinate placed at CII = 37 places most of the cloud contaminated cells to the left (i.e. CII < 37.) and most of the uncontaminated cells to the right (i.e. CII > 37.0) (Refer to table 4.1 for and explanation of the cloud density codes.)

contaminated cells and the uncontaminated cells. This produced approximately 85 percent agreement between the CDC and the CII for both the July and October portions of this database; therefore, a threshold CII of 37.0 was used to identify cloud contaminated cells in the database. It is beyond the scope of this study to fine tune this threshold. Increasing the CII threshold will eliminate more cloud contaminated cells, but will also reduce, to a greater extent, the number of uncontaminated cells. Lowering the CII threshold will increase the number of uncontaminated cells and also increase the number of contaminated cells. When the EVI was plotted against the midcell pixel number associated with it to observe its distribution, both with and without the CII threshold of 37.0 being applied, it was noted that EVI's with associated midcell pixel numbers less than 200 failed to adhere to the conformity of the EVI's with midcell pixel numbers greater than 200. Therefore, an ancillary threshold on the midcell pixel number of 200 was incorporated\*. The effects of the two screening methods are illustrated in Figure 4.2a and Figure 4.2b. Figure 4.2a is a display of the EVI calculated from the July channel means against the midcell pixel number without any thresholds applied. The lack of EVI values less than two between midcell pixel numbers 500 and 1000 is due to the fact that the acquisitions collected when the study site was in the 500 to 1000 pixel number range were cloud free. Figure 4.2b displays the EVI's calculated

---

\*This scan line cut off, plus more drastic scan line cut backs are supported by Johnson (1983) and Horvath, et al, (1982).



ORIGINAL PAGE IS  
OF POOR QUALITY

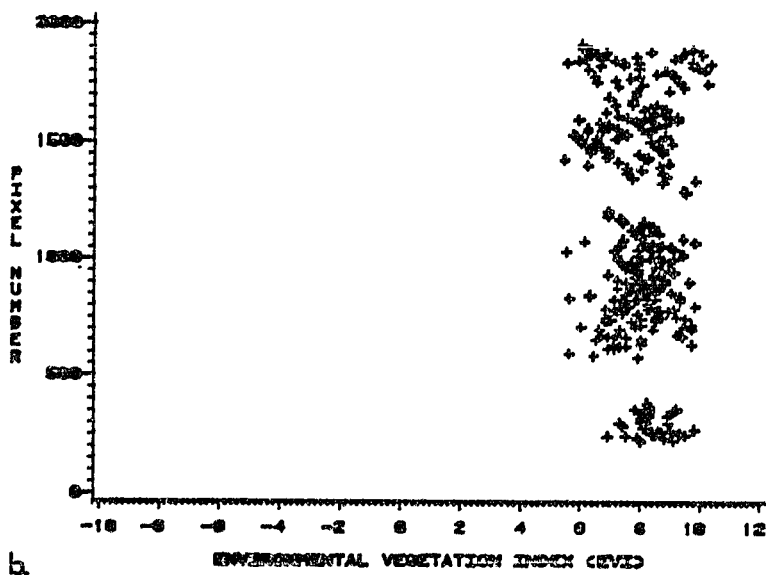
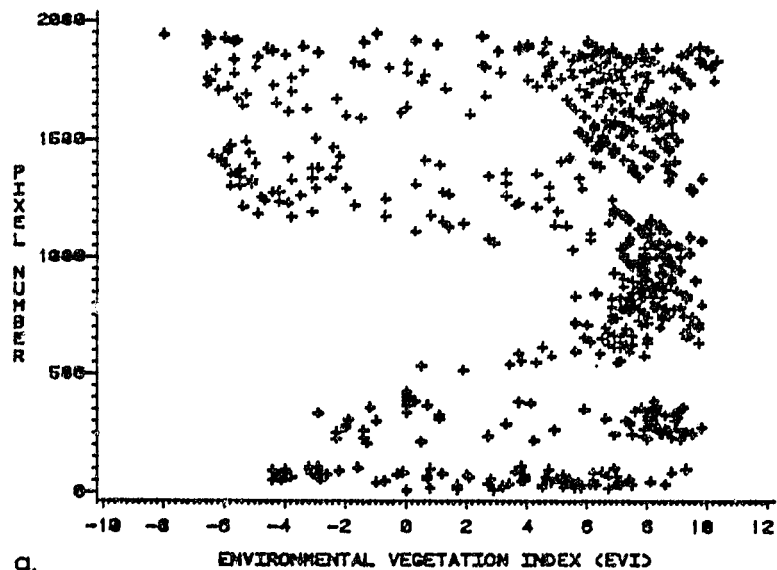


Figure 4.2 - (a) - a graph of midcell pixel numbers against EVI's calculated from the July channel means,  $n = 648$ ; (b) is the same July EVI values against midcell pixel numbers with a CII threshold of  $\leq 37.0$  and a midcell pixel number threshold of  $\leq 200$ ,  $n = 312$ . Notice the reduction of variability of the EVI in graph (b) compared to graph (a).

from the July channel means after the CII threshold of less than or equal to 37.0 and the midcell pixel number threshold of less than or equal to 200 was applied. It appears as though the CII threshold has the same effect as an EVI threshold of approximately five; however, this is not true. Grid cells with EVI's as high as nine were omitted due to the CII threshold. What appear to be gaps due to natural clustering of the EVI's along the scan line are due to lack of data, i.e. during these eight acquisitions the study site was not found along those portions of the scan line.

It is also interesting to note the effect of screening on the reflective and thermal channels themselves. Figure 4.3 is a plot of the reflectance in channel one against the reflectance in channel two before and after screening. In figure 4.3a, which is a plot before screening, the bulk of the data is clustered below 15 percent reflectance in channel two and below ten percent in channel one with a large "tail" of data trailing away from the cluster with increased reflectance. Figure 4.3b, which is a plot after screening techniques had been applied, illustrates how the bulk of the data of low reflectance remained and the tail of high reflectance data was omitted. Since natural terrestrial objects have relatively low reflectance in the reflective portion of the spectrum, this is a good indication that the screening techniques are identifying clouds and possibly hazy conditions which have a higher reflectance than natural terrestrial objects. This figure (4.3) may support an argument to screen (threshold) data based on channel one reflectance of approximately 9 or 10 percent. Since the channel two reflectance varies during a growing season according to the amount of green biomass present, a similar argument cannot be made using channel two.

ORIGINAL PAGE IS  
OF POOR QUALITY

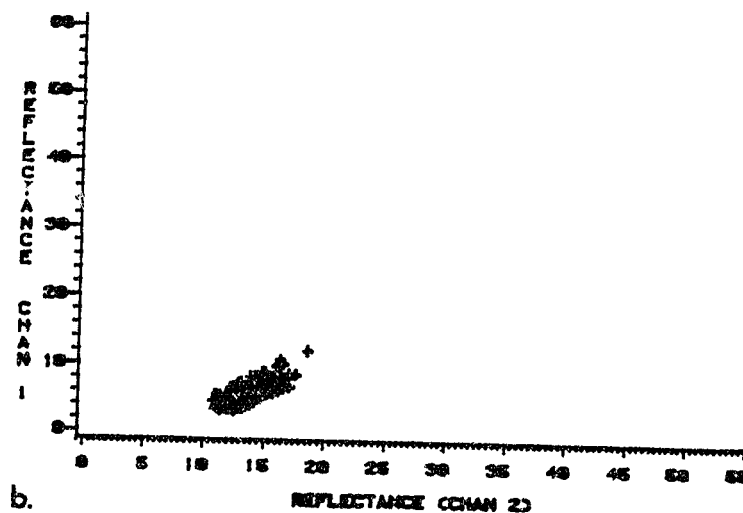
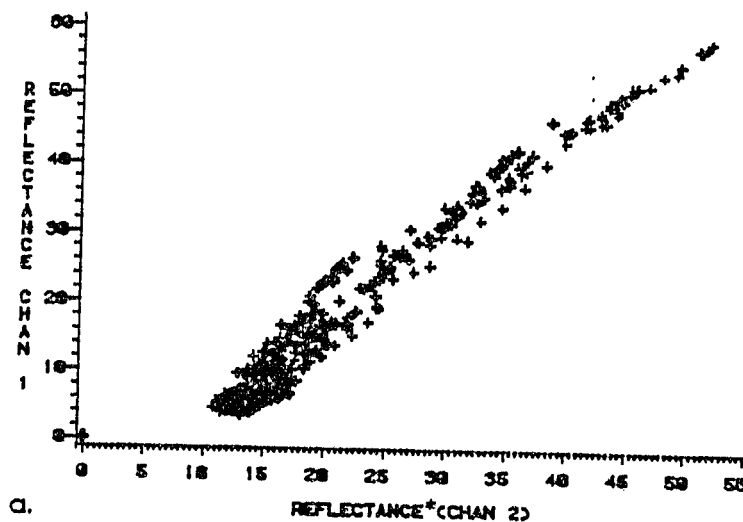


Figure 4.3 - plots of the July channel 1 cell means against channel 2 cell means without (a) and with (b) thresholds of  $CII \leq 37$  and midcell pixel numbers  $\leq 200$ . Notice how the bulk of the tightly clustered data with low reflectance in Channels 1 and 2 remained after thresholds were applied and the less clustered more amalgamous data has been omitted.

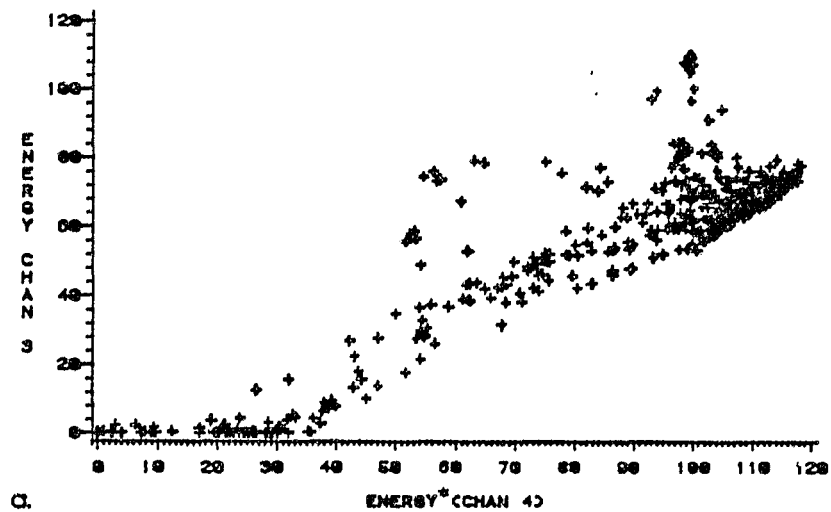
\*reflectance - percent albedo.

Figure 4.4 is a plot similar to figure 4.3 except that the thermal channels are plotted against each other in energy ( $\text{mWm}^{-2} \text{ sr cm}$ ). The results in the thermal channels are similar to the reflective channels in eliminating the amalgamous data present (Fig. 4.4a) and leaving behind the bulk of the clustered data after screening (fig. 4.4b). The amalgamous data for the most part is colder and wetter, which for the most part are clouds or atmospheric haze.

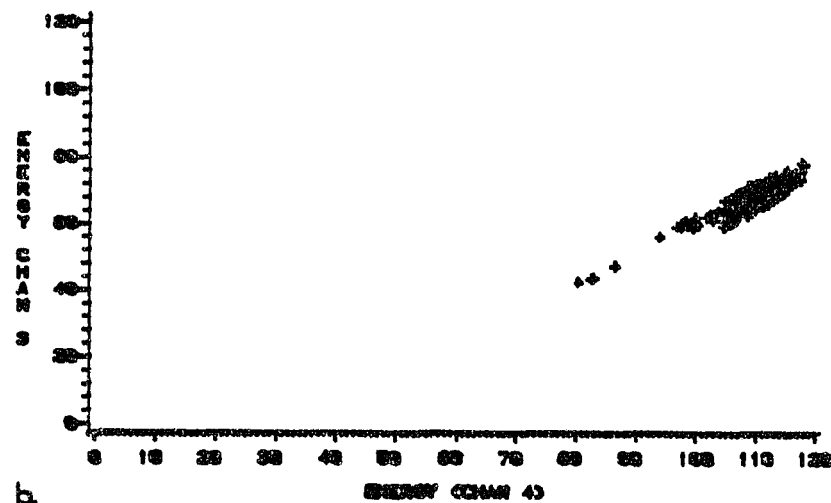
#### 4.2 Effects of Solar Correction/Standardization on the EVI

The information content of the EVI can be significantly altered by applying solar corrections and/or standardization techniques. In figure 4.5 the EVI,  $\text{EVI}_{\text{corr}}$ , and  $\text{EVI}^*$  are calculated from the July data and are plotted against the midcell pixel number to illustrate the changes in the EVI and its derivations along a scan line. A scan line also has a constantly changing solar zenith angle associated with it. The solar corrected and standardized EVI, the  $\text{EVI}^*$  (fig 4.5c), is extremely biased. For example, it would be impossible to obtain an  $\text{EVI}^*$  less than 20 when the midcell pixel number is less than 500. Nearly any EVI value within the dynamic range of EVI's (fig. 4.5a) can be obtained regardless of midcell pixel number. The  $\text{EVI}^*$ , which is supposed to be an indication of vegetal conditions, is more dependent on satellite positions (or its solar zenith angles) than it is on actual ground conditions.

ORIGINAL TABLES  
OF POOR QUALITY



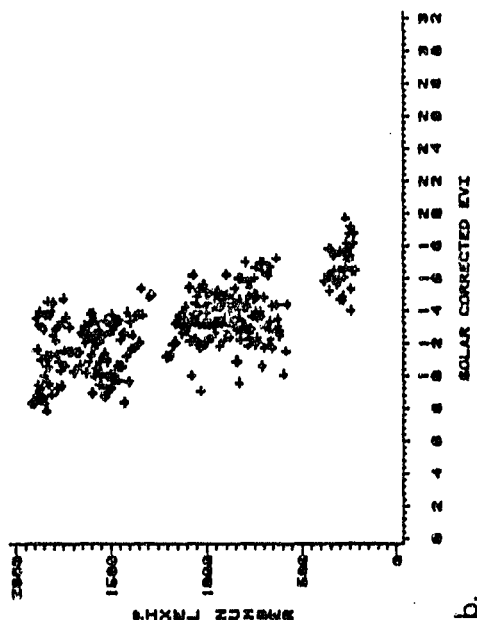
a.



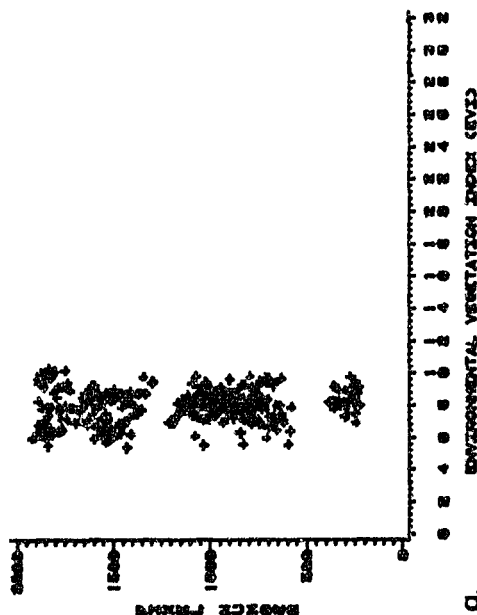
b.

Figure 4.4 - plots of the July channels 3 cell means against channel 4 cell means without (a) and with (b) thresholds of  $CII \leq 37$  and mid-cell pixel numbers  $\leq 200$ . Notice how the bulk of the tightly clustered data remained after the thresholds were applied and the amalgamous data has been omitted.

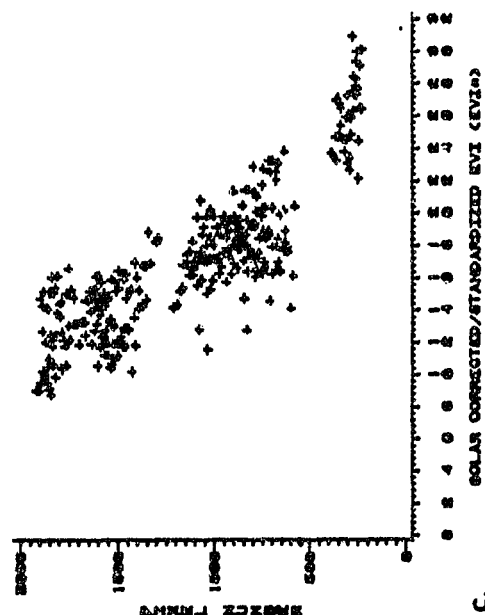
\* energy -  $\text{mWm}^{-2} \text{ sr cm}$



b.



c.



d.

Figure 4.5 - These plots show the EVI plotted against the midcell pixel number to illustrate the distribution changes as different solar correction/standardization techniques are applied. All plots use the screened July data for illustration. The EVI is uncorrected and unstandardized in (a); the standard Landsat MSS correction ( $1/\cos \theta$ ) has been applied in (b); and the EVI has been solar corrected and standardized to  $39^\circ$  in (c). Note how the EVI becomes increasingly more biased as corrections and standardizations are applied.

Using simple linear regression to model EVI and EVI\* against the midcell pixel number, a coefficient of correlation ( $R^2$ ) can be calculated which measures the amount of the error explained by the model. In the case of an indicator index, the model's independent variables should be independent (uncorrelated) of the index (dependent variables). When the midcell pixel number is used to model the EVI\* the coefficient of correlation was 75 percent which could be broadly interpreted as an indication that the midcell pixel number is nearly as good as the EVI\* at indicating vegetal conditions. When the EVI is regressed on the midcell pixel number an  $R^2$  value of two percent was obtained indicating the EVI is independent (uncorrelated) to the mid cell pixel number.

#### 4.3 Mean and Variance Equality Tests

Based on the assumptions described in Section 1.3, it is not likely that an IJ grid cell (approximately 530,000 acres) would have a significant change in illumination or reflectance properties between acquisitions, approximately 24 hours. Under these assumptions the scene means and variances would be more or less identical from one day to the next. This is not the case. The biggest impact on the daily means and variances is due to clouds and other atmospheric interferences as shown in figure 4.6. This figure shows the results of tests of equality of scene means and variances of all July EVI values. After applying the CII threshold and midcell pixel number threshold to the July EVI scene means and variances, there is an approximately 30 percent increases in the percentage of scene means and variances which do not exhibit a significant difference, as shown in figure 4-7.

192	193	194	195a	195b	196	197	Day
NS	*	NS	NS	NS	*	*	191
	*	NS	NS	NS	*	*	192
		*	*	*	*	*	193
			NS	*	*	*	194
				*	*	*	195a
					*	*	195b
						*	196

a. Results from the test of variance equality.

192	193	194	195a	195b	196	197	Day
NS	*	NS	NS	NS	*	*	191
	*	NS	NS	NS	*	*	192
		*	*	*	NS	*	193
			NS	NS	*	*	194
				*	*	*	195a
					*	*	195b
						*	196

b. Results from the test of mean equality.

Figure 4.6 - The above tables show the results from the tests of equality between variances (a) and means (b) at the  $\alpha = 0.05$  level of significance for unscreened and uncorrected EVI's in July, 1980. Note: \* - indicates means or variances are significantly different and the null hypothesis of equality should not be accepted; NS - denotes no significant difference and the null hypothesis should be accepted.



192	193	194	195a <sup>1</sup>	195b	196	197	Day
NS	NS	NS		*	NS	NS	191 <sup>2</sup>
	NS	NS		NS	NS	NS	192 <sup>2</sup>
		*		*	NS	*	193
				*	*	NS	194
							195a
					*	*	195b
						*	196

a. Results from the test of variance equality.

192	193	194	195a	195b	196	197	Day
NS	NS	*		*	NS	NS	191
	NS	*		NS	NS	*	192
		*		NS	NS	*	193
				NS	*	NS	194
							195a
					NS	NS	195b
						*	196

b. Results from the test of mean equality.

Figure 4.7 - The above tables show the results from the tests of equality between variances (a) and means (b) at the  $\alpha = 0.05$  level of significance for screened and uncorrected EVI's in July, 1980.  
Note: \* - indicates means or variances are significantly different and the null hypothesis of equality should not be accepted; NS - denotes no significant difference and the null hypothesis should be accepted.

<sup>1</sup> - all IJ grid cells during this observation had pixel numbers less than 200.

<sup>2</sup> - day 191 and 192 had 3 and 6 observations respectively after screening.

The screening methods discussed in this section improve the reliability of the EVI as seen in the means in figure 4-8 and the variances in table 4-2. These types of improvements in information content of data are necessary in operational databases or in studies requiring comparisons temporally, such as large scale change monitoring.

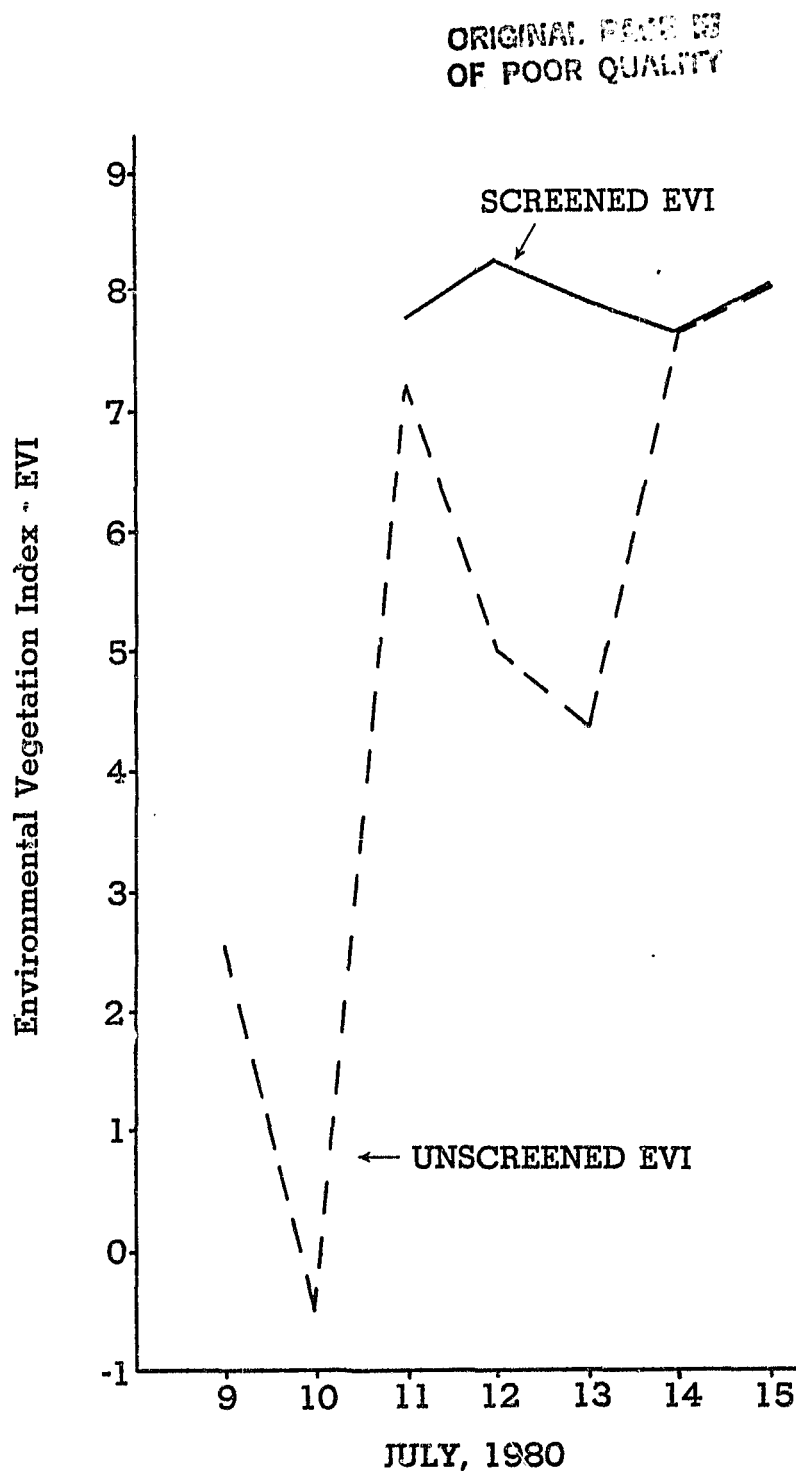


Figure 4-8. A plot of screened and unscreened scene mean EVI's over the Illinois study site by date for the July data only. July 9th and 10th screened EVI's are not plotted as only 3 and 6 observations, respectively, were left after screening.

Table 4-2. This table is a summary of descriptive statistics for the three types of unscreened (a) and screened (b) EVI VIN's for the July observations, over Illinois.

(a) Unscreened

VIN	MIN	MAX	MEAN	VAR	N
EVI	-8.0	10.3	4.65	21.39	648
EVI <sub>corr</sub>	-10.9	20.5	8.10	61.38	636
EVI*	-18.8	38.1	10.98	121.99	636

(b) Screened

VIN	MIN	MAX	MEAN	VAR	N
EVI	5.4	10.3	7.94	1.04	312
EVI <sub>corr</sub>	7.8	19.7	13.18	5.36	312
EVI*	8.7	30.9	17.20	20.92	312

## 5.0 LITERATURE CITED

- Boatwright, G. O. 1981. Early Warning/Crop Condition Assessment. Project Implementation Plan. USDA-ARS, Houston, Texas.. 175 p.
- Cate, R. B., J. A. Artley and D. E. Phinney. 1980. Quantitative Estimation of Plant Characteristics Using Spectral Measurements: A Survey of the Literature. Lockheed Engineering and Management Services Co., Inc. Houston, Texas. LEMSCO-14077, 42 p.
- Charney, J. G. and N. A. Phillips. 1953. Numerical Integration of the Quasi-Geostrophic Equations for Barotropic and Simple Baroclinic Flows. J. Meteor. 10(2):71-99.
- Gray, T. I. and D. G. McCrary, 1981. The Environmental Vegetation Index. A Tool Potentially Useful for Arid Land Management. NOAA/NESS/ESL Land Sciences Branch. Houston, Texas. EW-N1-04076. 5 p.
- Gray, T. I., D. G. McCrary and T. A. Armstrong. 1981. Characteristics of TIROS, GOES, DMSP and Landsat Systems. NOAA/USDC Houston, Texas. EW-N1-04075, 17 p.
- Horvath, N. C., T. I. Gray and D. G. McCrary. 1982. Advanced Very High Resolution Radiometer for use in Monitoring Vegetation, Volume I - Channels 1 and 2. Lockheed Engineering and Management Services Co., Inc., Houston, Texas. LEMSCO-17383, 94 p.
- Johnson, W. R., 1983. Atmospheric Effects on Metsat Data. Lockheed Engineering and Management Services Co., Inc., Houston, Texas. LEMSCO-18836.
- National Aeronautics and Space Administration. 1982. FY1981 AgRISTARS Annual Report, NASA-JSC, Houston, Texas AP-J2-04225, 59 pp.
- National Aeronautics and Space Administration. 1978. Large Area Crop Inventory Experiment (LACIE) Phase I and Phase II Accuracy Assessment Final Report. NASA-JSC, Houston, Texas, JSC-13736.